A feasibility study using an array of $LaBr_3$(Ce) scintillation detectors as a Compton camera for prompt gamma imaging during BNCT

K. Nutter, T. Price, Tz. Kokalova, S. Green, B. Phoenix.

Corresponding email: kjn718@bham.ac.uk

UNIVERSITY OF BIRMINGHAM

EPSRC CENTRE FOR DOCTORAL TRAINING
TOPOLOGICAL DESIGN

ORIGINAL RESEARCH article

Front. Phys., 21 February 2024
Sec. Medical Physics and Imaging
Volume 12 - 2024 | https://doi.org/10.3389/fphy.2024.1347929

This article is part of the Research Topic
Prompt-gamma Imaging in Particle Therapy
View all 3 Articles >

A feasibility study using an array of $LaBr_3$(Ce) scintillation detectors as a Compton camera for prompt gamma imaging during BNCT

Kiran Nutter[1]* Tony Price[1] Tzany Kokalova[1] Stuart Green[1,2] Ben Phoenix[1]

[1] School of Physics and Astronomy, University of Birmingham, Birmingham, United Kingdom
[2] Queen Elizabeth Hospital Birmingham, University Hospitals Birmingham NHS Foundation Trust, Birmingham, United Kingdom

Corresponding email: kjn718@bham.ac.uk

Boron Neutron Capture Therapy (BNCT)

- Binary cancer therapy that utilises biological and physical targeting of the tumour

- Neutron capture produces short-range, high linear energy transfer (LET) particles

- Research has focused on brain, head and neck cancers

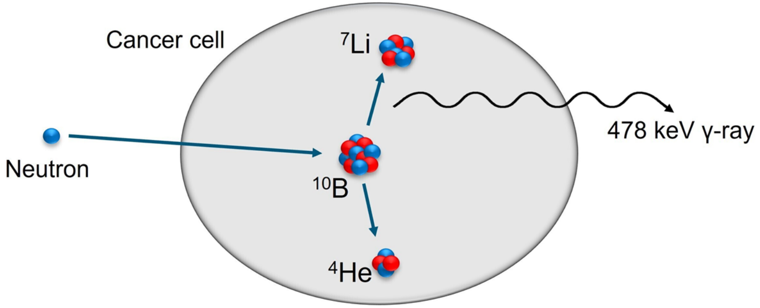

Fig 1. Visual representation of the fundamental interaction utilised during BNCT.

- Cross section for thermal neutron capture on ^{10}B is 3840 barns [1]

[1] D. A. Brown et al. ENDF/B-VIII.0: The 8th Major Release of the Nuclear Reaction Data Library with CIELO-project Cross Sections, New Standards and Thermal Scattering Data, Nucl. Data Sheets, 148:1-142 (2018).

Boron Neutron Capture Therapy (BNCT)

ay

However, obtaining accurate dosimetry is challenging!!!

neutron capture on ^{10}B is 3840 barns [1]

- Research has focused on brain, head and neck cancers

[1] D. A. Brown et al. ENDF/B-VIII.0: The 8th Major Release of the Nuclear Reaction Data Library with CIELO-project Cross Sections, New Standards and Thermal Scattering Data, Nucl. Data Sheets, 148:1-142 (2018).

Prompt Gamma Imaging for BNCT

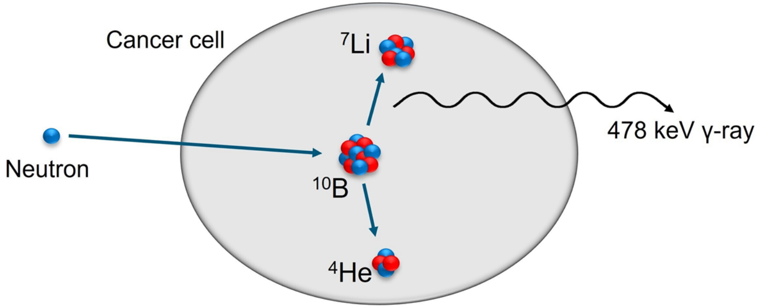

Fig 1. Visual representation of the fundamental interaction utilised during BNCT.

Prompt Gamma Imaging for BNCT

- A 478 keV prompt gamma ray is produced after 93.9% of the neutron capture interactions

- Delivered dose could be inferred by imaging the production vertices of these gamma rays

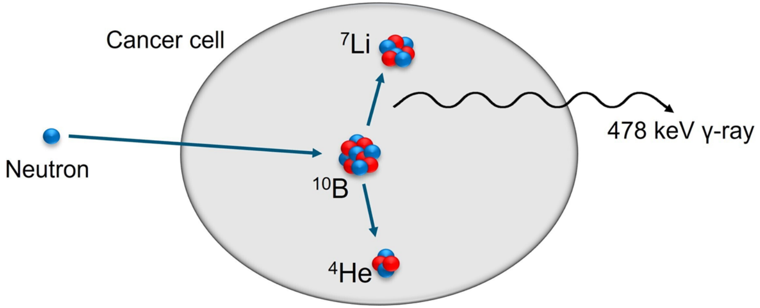

Fig 1. Visual representation of the fundamental interaction utilised during BNCT.

$$^{10}B + n \rightarrow {}^{7}Li + \alpha + 2.79\ \text{MeV} \quad (6.1\%)$$

$$^{10}B + n \rightarrow {}^{7}Li^{*} + \alpha + 2.31\ \text{MeV} \quad (93.9\%)$$

$$^{7}Li^{*} \rightarrow {}^{7}Li + \boxed{\gamma\ (0.478\ \text{MeV})}$$

Prompt Gamma Imaging for BNCT

- A 478 keV prompt gamma ray is produced after 93.9% of the neutron capture interactions

- Delivered dose could be inferred by imaging the production vertices of these gamma rays

- Imaging could be done with SPECT or Compton camera systems

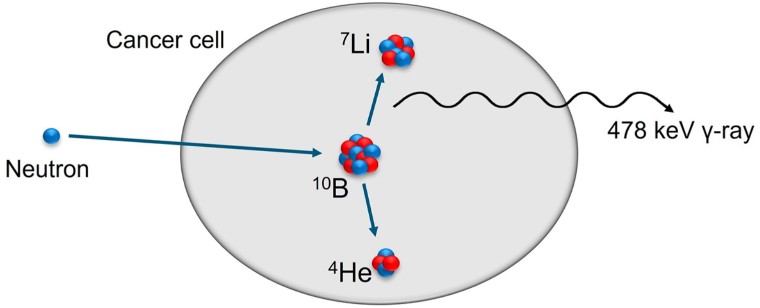

Fig 1. Visual representation of the fundamental interaction utilised during BNCT.

$$^{10}\mathbf{B} + \mathbf{n} \rightarrow {}^{7}\mathbf{Li} + \alpha + 2.79\ \mathbf{MeV} \quad (6.1\%)$$

$$^{10}\mathbf{B} + \mathbf{n} \rightarrow {}^{7}\mathbf{Li}^{*} + \alpha + 2.31\ \mathbf{MeV} \quad (93.9\%)$$

$$^{7}\mathbf{Li}^{*} \rightarrow {}^{7}\mathbf{Li} + \boxed{\gamma\ (0.478\ \mathbf{MeV})}$$

Compton Camera

- Combining the axis between the two interaction points with the calculated scattering angle, we obtain a conical surface from which the photon must have originated

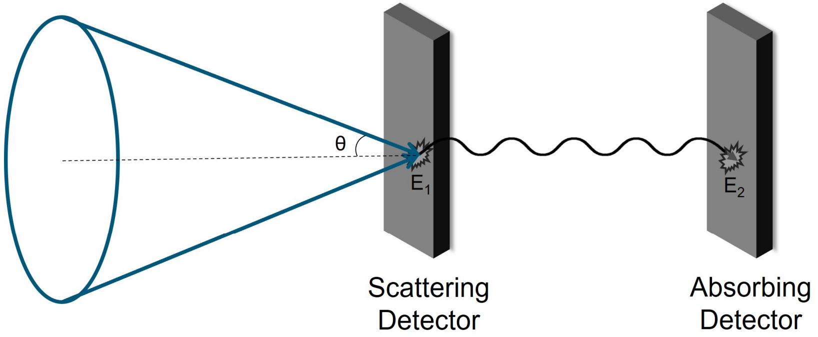

Fig 2. Principle of operation of a Compton camera.

Compton scattering equation

$$\cos\theta = 1 - \frac{m_e c^2 E_1}{E_2(E_1 + E_2)}$$

Compton Camera

- Combining the axis between the two interaction points with the calculated scattering angle, we obtain a conical surface from which the photon must have originated

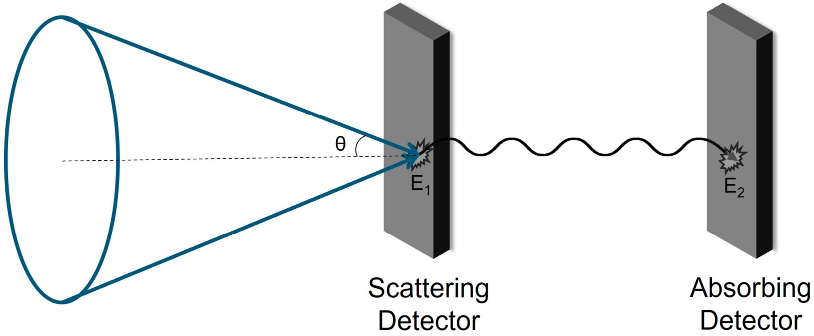

Fig 2. Principle of operation of a Compton camera.

<u>Compton scattering equation</u>

$$\cos\theta = 1 - \frac{m_e c^2 E_1}{E_2(E_1 + E_2)}$$

- Does not rely on mechanical collimation of photons like a SPECT system

$LaBr_3$ Detector Array

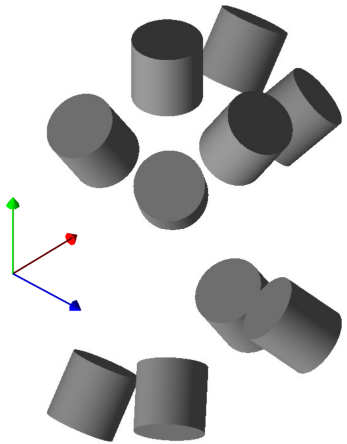

Fig 3. Original 10 detector array.

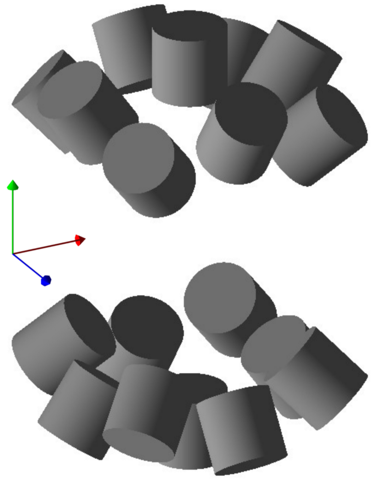

Fig 4. Extrapolated 18 detector array.

$LaBr_3$ Detector Array

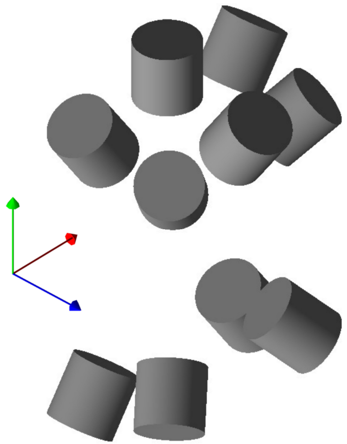

Fig 3. Original 10 detector array.

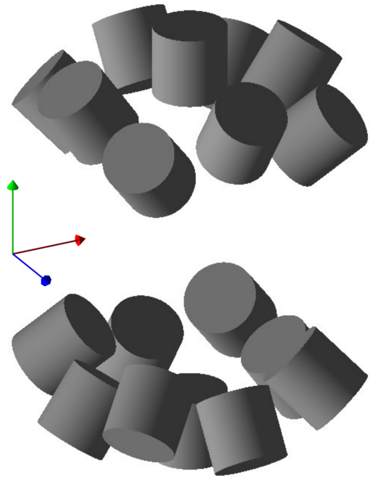

Fig 4. Extrapolated 18 detector array.

- Each detector can act as a scattering and absorbing detector
- Requires large angle scatters

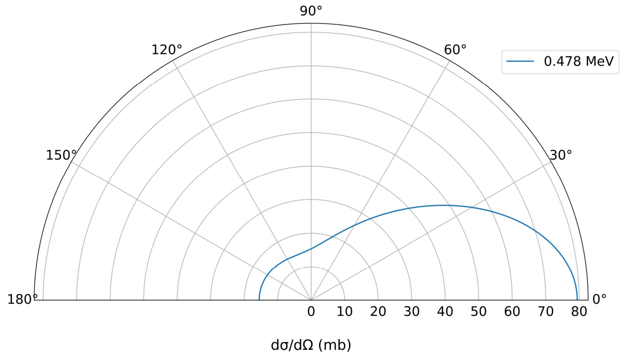

Fig 5. Klein-Nishina distribution for a 478 keV photon.

Modified Compton Camera Advantages

- Significantly increases the number of detection channels

Detection channel - a distinct pair of a scattering and absorbing detector.

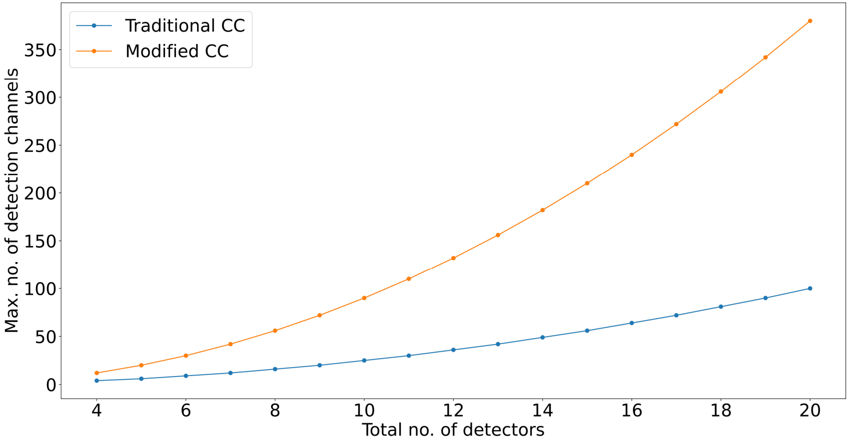

Fig 6. Max. detection channels achieved when using a traditional and modified Compton camera design.

Modified Compton Camera Advantages

- Significantly increases the number of detection channels
- This increase helps to counteract lower scattering probability
- Greater variety of cones produced should improve spatial resolution

Detection channel - a distinct pair of a scattering and absorbing detector.

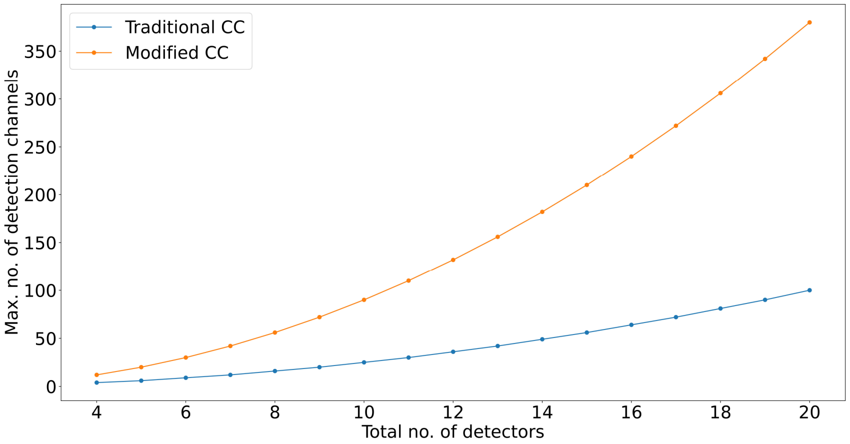

Fig 6. Max. detection channels achieved when using a traditional and modified Compton camera design.

Simulation Design

- Initial testing and validation using 478 keV point source
- Then introduced neutron beam and phantom
- Tumour contained 400 ppm ^{10}B

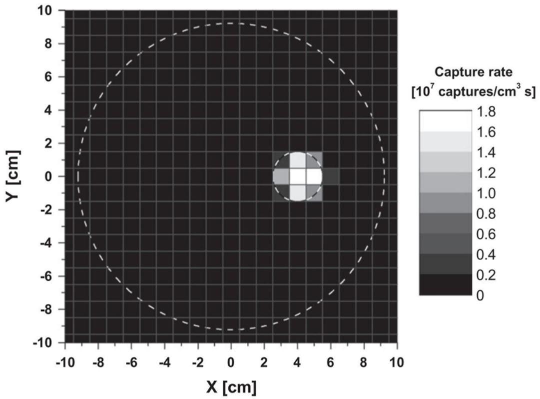

Fig 7. Tomographic image of boron neutron capture rate from Minsky et al [2].

[2] D. Minsky, A. Valda, A. Kreiner, S. Green, C. Wojnecki, Z. Ghani. First tomographic image of neutron capture rate in a BNCT facility, Appl. Rad. Iso. 69:1858-61 (2011).

Simulation Design

- Initial testing and validation using 478 keV point source
- Then introduced neutron beam and phantom
- Tumour contained 400 ppm ^{10}B

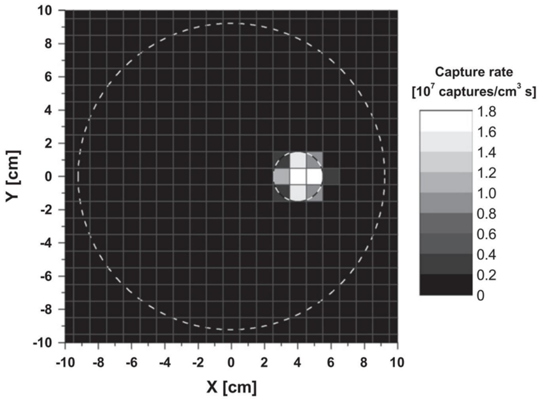

Fig 7. Tomographic image of boron neutron capture rate from Minsky et al [2].

- The effect of different shielding types also tested

- Pb and ^{6}Li shielding were tested one at a time

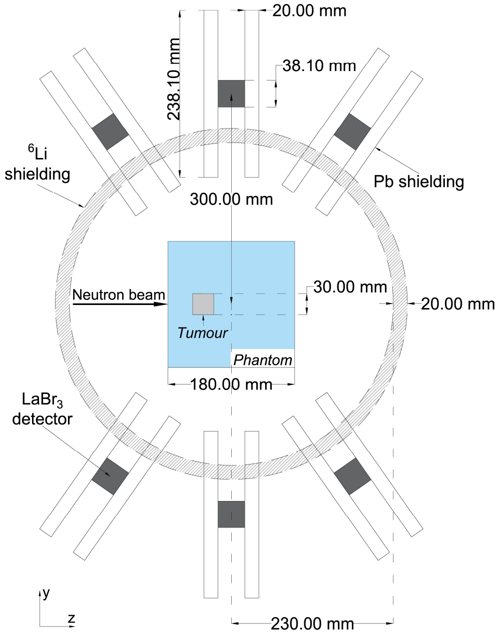

Fig 8. Schematic diagram of simulated setup, with both shielding types included.

[2] D. Minsky, A. Valda, A. Kreiner, S. Green, C. Wojnecki, Z. Ghani. First tomographic image of neutron capture rate in a BNCT facility, Appl. Rad. Iso. 69:1858-61 (2011).

Shielding Investigation – ^{6}Li Neutron Shielding

- Labelled peaks were expected to be the most prominent
- But, minimal 511 keV contribution and many unexpected peaks

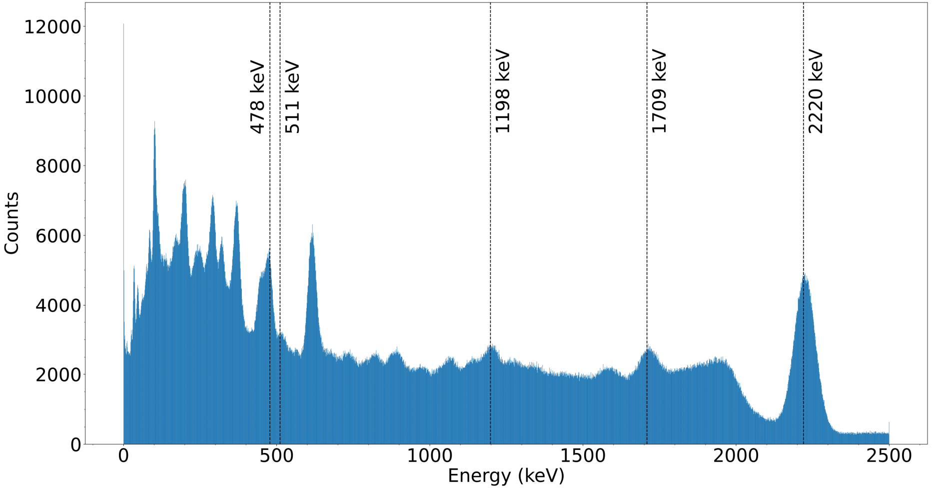

Fig 9. Gamma spectrum for a detector in the array **with no shielding included.**

Shielding Investigation – ^{6}Li Neutron Shielding

- Labelled peaks were expected to be the most prominent
- But, minimal 511 keV contribution and many unexpected peaks
- Most of the additional structure was removed when adding neutron shielding

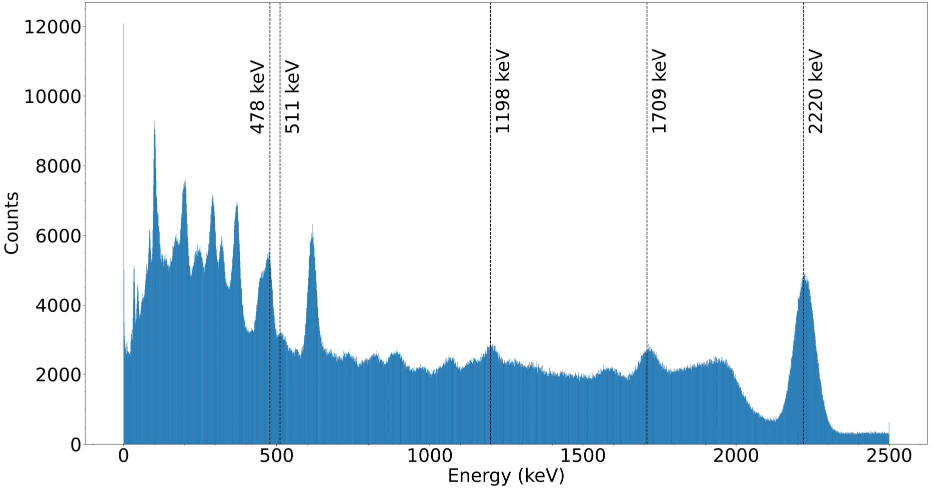

Fig 9. Gamma spectrum for a detector in the array **with no shielding included.**

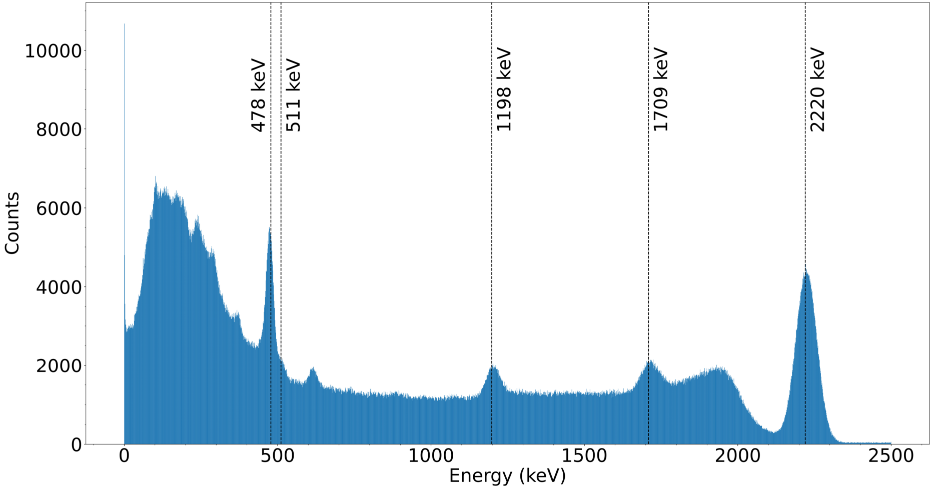

Fig 10. Gamma spectrum for the same detector **with ^{6}Li neutron shielding included.**

Shielding Investigation – Pb gamma shielding

- Neutron shielding was removed to test effect of the Pb alone

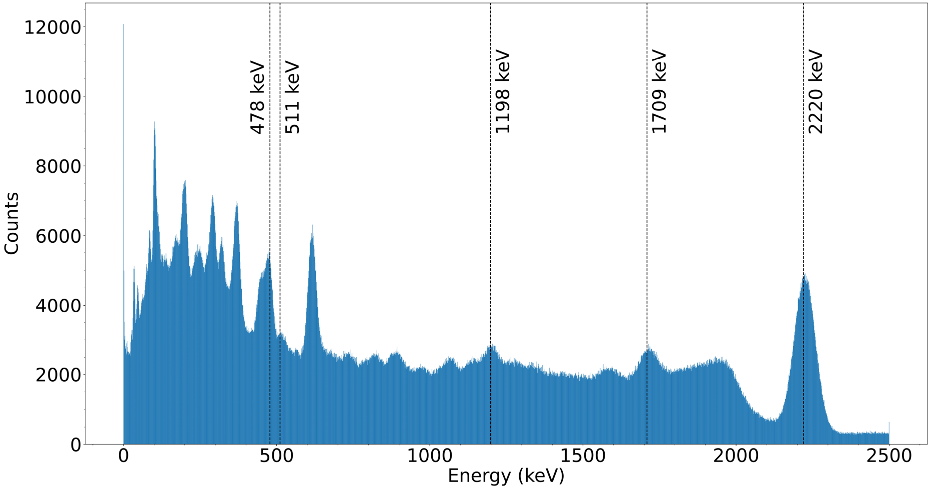

Fig 9. Gamma spectrum for a detector in the array **with no shielding included.**

Shielding Investigation – Pb gamma shielding

- Neutron shielding was removed to test effect of the Pb alone
- 511 keV peak now much more prominent – primarily created in shielding

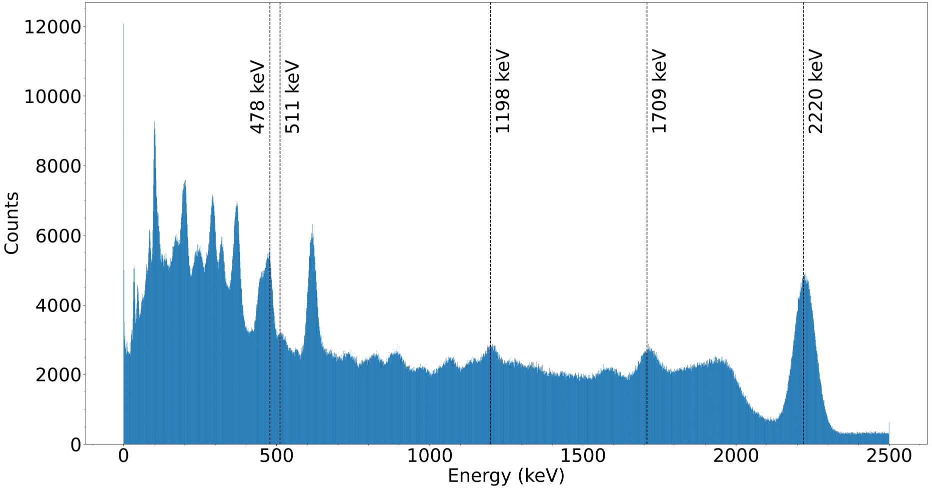

Fig 9. Gamma spectrum for a detector in the array **with no shielding included.**

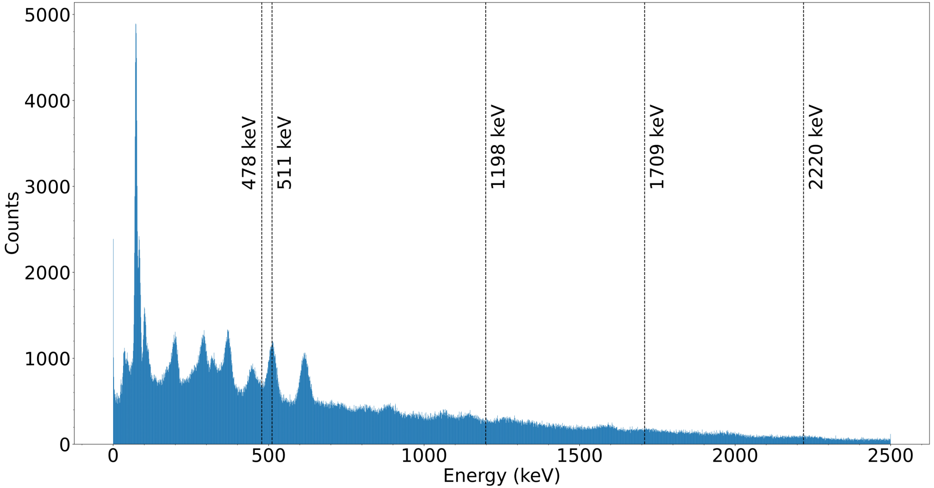

Fig 11. Gamma spectrum for the same detector **with Pb gamma shielding included.**

Shielding Investigation – Pb gamma shielding

- Neutron shielding was removed to test effect of the Pb alone
- 511 keV peak now much more prominent – primarily created in shielding
- **Reduced shielding requirements of Compton camera could benefit imaging 478 keV photons!**

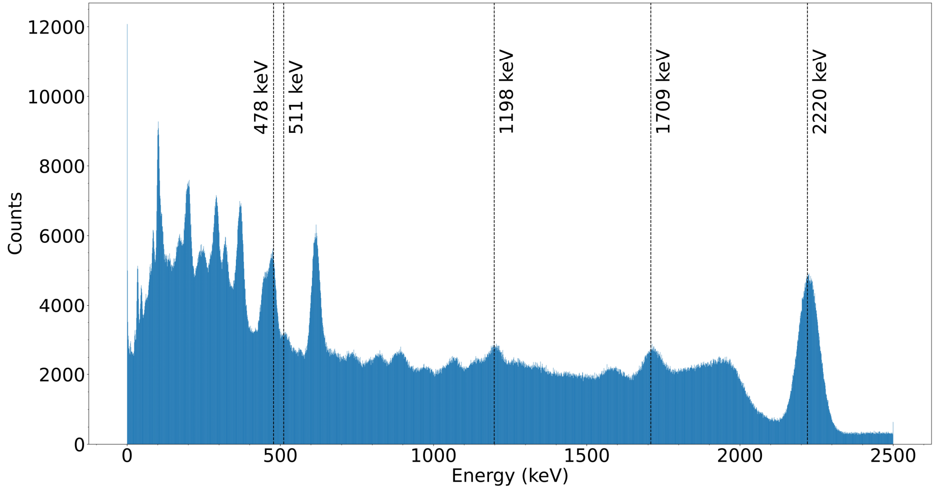

Fig 9. Gamma spectrum for a detector in the array **with no shielding included.**

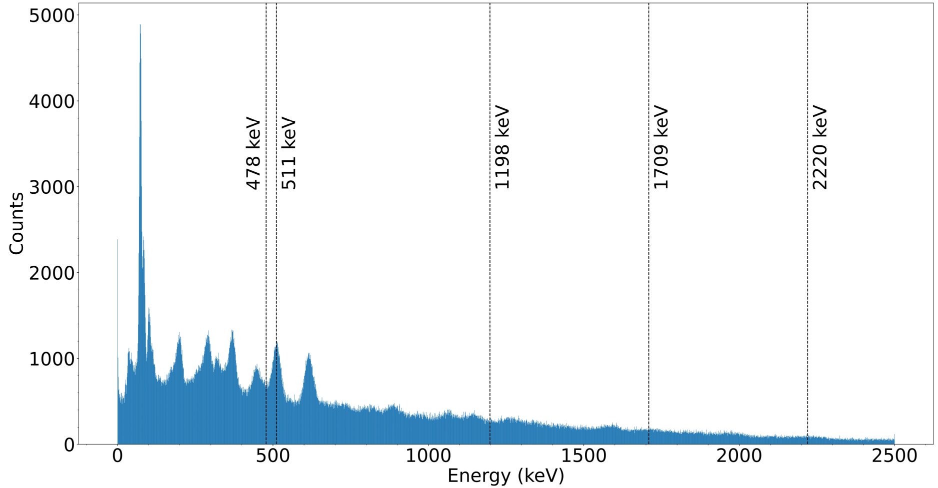

Fig 11. Gamma spectrum for the same detector **with Pb gamma shielding included.**

Reconstructed Images of Testing Phantom

- True source of the 478 keV photons extracted from simulation

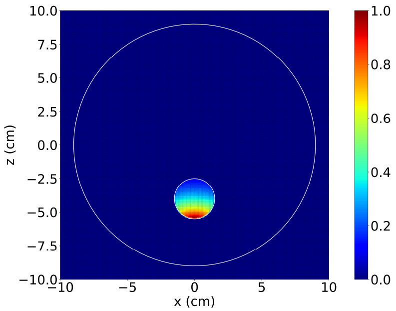

Fig 12. True distribution of origin of 478 keV gamma rays.

Reconstructed Images of Testing Phantom

- True source of the 478 keV photons extracted from simulation

- Reconstructed image clearly highlights the tumour region – highest intensity at bottom edge

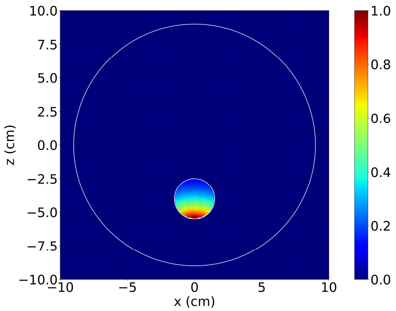

Fig 12. True distribution of origin of 478 keV gamma rays.

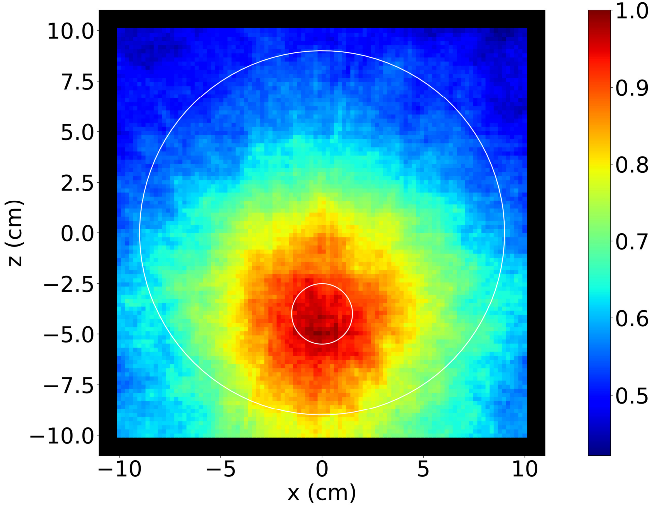

Fig 13. Reconstructed image of the origin of the 478 keV gamma rays.

Reconstructed Images of Testing Phantom

- True source of the 478 keV photons extracted from simulation
- Reconstructed image clearly highlights the tumour region – highest intensity at bottom edge
- 0.004% absolute efficiency
- Further study would be required to quantify spatial resolution

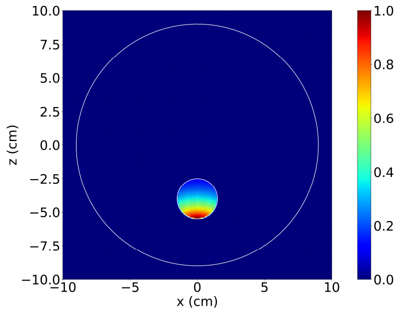

Fig 12. True distribution of origin of 478 keV gamma rays.

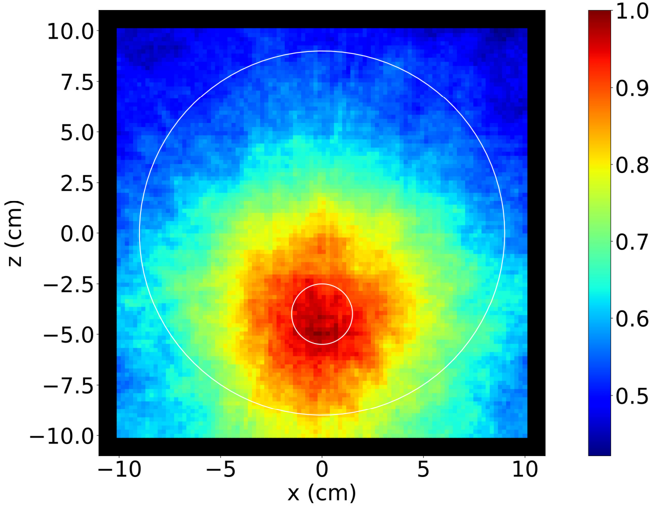

Fig 13. Reconstructed image of the origin of the 478 keV gamma rays.

Next Steps

- Consider increased complexity when making clinically viable
- Optimise camera geometry
- Extract reliable dose information from reconstructed images
- Feasibility measurements at the High-Flux Accelerator-Driven Neutron Facility at the University of Birmingham

UNIVERSITY OF BIRMINGHAM
HIGH FLUX ACCELERATOR-DRIVEN NEUTRON FACILITY

Summary

- BNCT provides alternative cancer therapy with both biological and physical targeting of the tumour
- Dosimetry is challenging, but prompt gamma imaging could offer an online method

- Feasibility study of using modified Compton camera for prompt gamma imaging during BNCT was carried out with Geant4
- **Using an epithermal neutron beam and phantom, the source of 478 keV photons was successfully identified**

UNIVERSITY OF
BIRMINGHAM

EPSRC CENTRE FOR DOCTORAL TRAINING
TOPOLOGICAL
DESIGN

Effect of ^{6}Li shielding on coincidence spectra

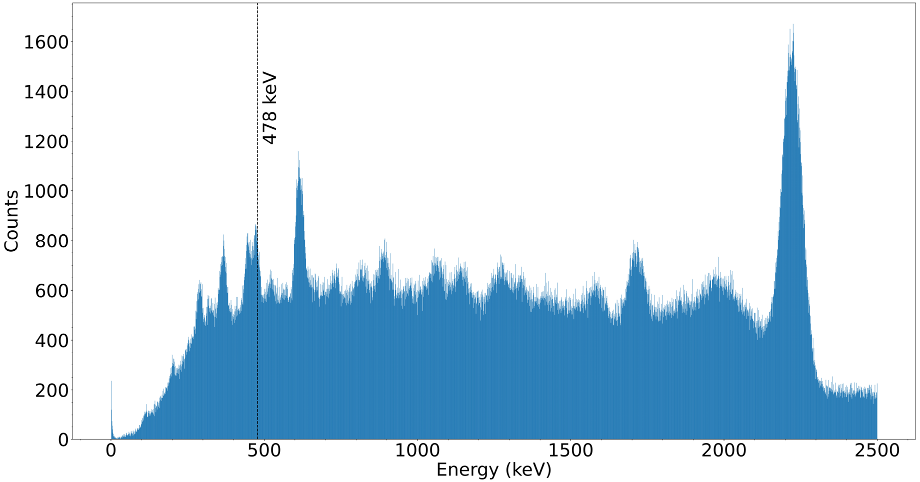

Spectrum of summed energies from all coincidence events, **with no neutron shielding.**

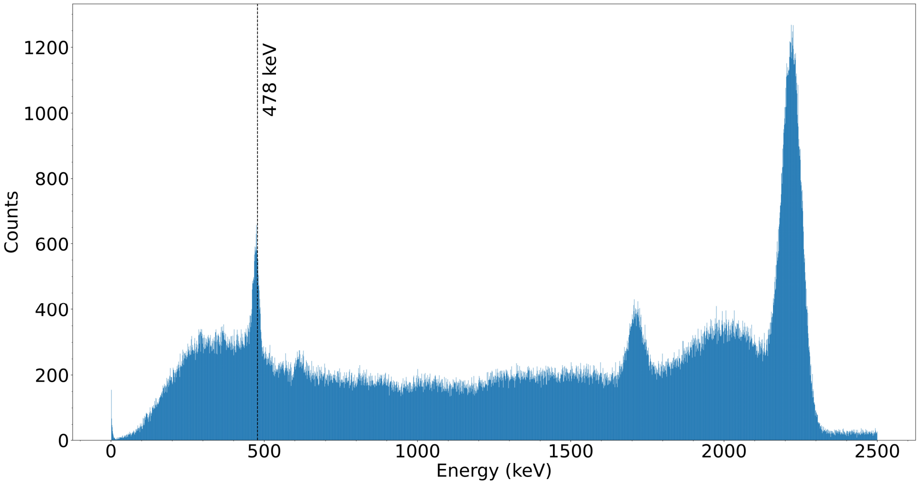

Spectrum of summed energies from all coincidence events, **with ^{6}Li neutron shielding.**

Contours of sensitivity correction factor